

1 **Optimising sampling design for the genomic analysis of**
2 **quantitative traits in natural populations**

3
4 Jefferson F. Paril¹, David J. Balding^{1,2,3}, Alexandre F. Fournier-Level^{1,2}

5 ¹School of Biosciences, ²Melbourne Integrative Genomics, and ³School of Mathematics and
6 Statistics, The University of Melbourne, Parkville 3010, Australia

7
8 **Author for correspondence:** Alexandre Fournier-Level (afournier@unimelb.edu.au)

9
10 **Keywords:** genome-wide association, individual sequencing, landscape genomics, pool
11 sequencing, genomic prediction, simulation

13 **Abstract**

14 Mapping the genes underlying ecologically-relevant traits in natural populations is fundamental
15 to develop a molecular understanding of species adaptation. Current sequencing technologies
16 enable the characterisation of a species' genetic diversity across the landscape or even over its
17 whole range. The relevant capture of the genetic diversity across the landscape is critical for a
18 successful genetic mapping of traits and there are no clear guidelines on how to achieve an
19 optimal sampling. Here we determine through simulation, the sampling scheme that maximises
20 the power to map the genetic basis of a complex trait across an idealised landscape and draw
21 genomic predictions for the trait, comparing individual and pool sequencing strategies. Our
22 results show that QTL detection power and prediction accuracy are higher when performing a
23 shallow sampling of more populations over the landscape which is done best using pool
24 sequencing. Populations should be collected from areas of high genetic diversity and we
25 recommend against sampling from the margins of the species' range. As progress in sequencing
26 enables the integration of trait-based functional ecology into landscape genomics studies, these
27 findings will guide study designs allowing direct measures of genetic effects in natural
28 populations across the environment.

29

30 **Introduction**

31 Connecting a species' molecular variation to functional traits is a central goal in ecology.
32 Genomic information for a species can then be leveraged to understand and eventually predict
33 population fitness under a range of eco-evolutionary scenarios. Unfortunately, the required
34 genotype-to-phenotype map is only available for a handful of traits, and primarily in model
35 organisms. With the improved accessibility of sequencing technologies, genome-wide

36 association studies (GWAS) and genomic prediction (GP) are becoming straightforward
37 approaches to understand and predict complex traits (Gondro et al., 2013). We thus coined the
38 term GPAS (Genomic Prediction and Association Studies) to denote genome-wide association
39 studies designed to both identify quantitative trait loci (QTL) and accurately predict traits from
40 genomic data. These studies rely on cost-effective, high-throughput sequencing and share the
41 same well-established linear modelling framework. However, how to sample natural populations
42 to train accurate GPAS models that are representative of the genetic diversity of a species is far
43 from obvious. More insights are needed to develop an optimal strategy and move away from *ad*
44 *hoc* field sampling.

45

46 Research in ecological genomics deals with the challenge of characterising the genetic basis of
47 traits across multiple natural populations. This requires collecting phenotype and genotype data
48 over the whole species' range which in practice, is often performed with limited resources. This
49 raises the problem of how to sample across a landscape to capture representative genetic
50 variation while constrained by the total sequencing depth attainable for a given budget. Here, we
51 address the question: how do we allocate a fixed sequencing capacity so that the genetic
52 information captured over the landscape leads to an optimal GPAS performance?

53

54 It is becoming easier to genotype genome-wide markers for large numbers of individuals, either
55 through whole-genome sequencing or complexity reduction approaches like restriction site-
56 associated DNA sequencing (RADseq) (Baird et al., 2008) for large complex genomes.
57 Increasing the density and number of markers for GPAS has the potential to increase QTL
58 detection power and prediction accuracy (de Roos et al., 2009; Long & Langley, 1999). Despite

59 the declining costs of sequencing, genotyping every individual of every population across a
60 landscape is usually not feasible, and phenotyping remains resource-consuming. As a cost-
61 effective alternative to sequencing individuals (Indi-seq), sequencing pools of individuals (Pool-
62 seq) (Schlötterer et al., 2014) has gained popularity in ecology (Bastide et al., 2013; Boitard et
63 al., 2012; Cheng et al., 2012; Nielsen et al., 2018), evolution (Boitard et al., 2012; Fracassetti et
64 al., 2015), and breeding (Beissinger et al., 2014; Bélanger et al., 2016) supported by
65 developments in quantitative genetics (Fournier-Level et al., 2017; Guo et al., 2018; Knight,
66 Saccone et al., 2009; Macgregor et al., 2006; Micheletti & Narum, 2018; Jinliang Yang et al.,
67 2015).

68

69 Indi-seq generates high-resolution genomic data of a population; while Pool-seq yields low-
70 resolution data in favour of cost reduction. Indi-seq yields individual allele information after
71 variant calling, while Pool-seq generates allele frequency estimates. Identifying when best to use
72 one over the other is important. Pool-seq has been shown to accurately capture genome-wide
73 allele frequencies (Fracassetti et al., 2015; Gautier et al., 2013; Rellstab et al., 2013; Zhu et al.,
74 2012), but is also prone to biases in genome representation when sample size and depth of
75 coverage are low (i.e. <40 individuals per pool and <50X depth) (Cutler & Jensen, 2010;
76 Schlötterer et al., 2014). Pool-seq also loses haplotype and linkage disequilibrium (LD)
77 information (Fariello et al., 2017) which limits the number of quantitative and population genetics
78 models that can be used and requires the design of novel analysis methods (Cutler & Jensen,
79 2010). Pool-seq is more cost-effective than Indi-seq (Futschik & Schlötterer, 2010; Gautier et al.,
80 2013), particularly for non-model organisms where individuals cannot be maintained indefinitely

81 and used in multiple experiments. Additionally, Pool-seq can include more individuals, grouped
82 into one or a few pools and sequenced at a high depth.

83

84 Field researchers often transfer techniques initially developed for model organisms or crops in
85 highly controlled environments; however, with natural populations having evolved in natural
86 environments this problem becomes non-trivial. Individuals and pools can be sampled from one
87 to a few populations or from a large number of populations. Identifying which populations
88 warrant higher resolution (Indi-seq instead of Pool-seq), requires some prior knowledge of the
89 spatial distribution of genetic variability across the landscape. To address this question, we
90 simulated landscapes under different trait architectures and population genetics scenarios with
91 the aim of providing recommendations on the optimal sampling strategies. Specifically, we aim to
92 answer the following three questions. How many populations do we need to sample to yield
93 optimal GPAS performance? Under which landscape-specific circumstances should we use Indi-
94 seq or Pool-seq? And which populations to select under different landscape scenarios?

95

96 **Materials and methods**

97 **Landscape simulations**

98 Variation for a quantitative phenotype over a landscape was simulated as a function of migration
99 rate, number of QTL controlling the trait, causal allele diffusion gradient, and selection intensity
100 with 3 levels for each of these parameters (Table 1).

101

102 Each landscape consisted of 100 populations arrayed in a uniform square lattice without
103 barriers. Migration was modelled using a 2-dimensional stepping-stone model with bidirectional
104 gene flow with a uniform rate into the 8 adjacent populations and absorbing boundaries.

105
106 The quantitative trait was determined by additive QTL with effects sampled from a χ^2 distribution
107 with 1 degree of freedom to generate a cumulated heritability of 0.5. At the initial step of the
108 simulation, all the causal alleles had a frequency (q_0) of 0.01 in the populations of origin and 0
109 elsewhere. Under the uniform allele diffusion gradient, all populations have $q_0=0.01$. Under the
110 unidirectional gradient, one boundary row has $q_0=0.01$ for all 10 populations in that row and 0
111 elsewhere. Under the bidirectional gradient, two opposite boundary rows have $q_0=0.01$ in each
112 of the populations and 0 elsewhere. For clarity, these causal allele diffusion gradients are
113 illustrated in Figure 1 Panel A.

114
115 Selection was simulated using a generalised logistic model (Richards, 1959) as

$$1/w = 1 + e^{y_c - y},$$

116
117 where w is fitness, y is the quantitative trait ($y \in \mathbb{R}$), $y_c = y_{min} + s(y_{max} - y_{min})$, with y_{max} and y_{min} the
118 maximum and minimum trait values, and s is the selection intensity.

119
120 The 10,000 biallelic loci were randomly distributed across a genome with 7 chromosomes and a
121 total length of 2×10^9 bases and 750 centimorgans to represent a large genome. The final (200th)
122 generation was sampled for the GPAS. Phenotypic values in this generation were scaled in the 0
123 to 1 interval for the GPAS experiments.

124

125 **Genome-wide association and trait prediction based on polygenic scores**

126 GPAS experiments were performed using Indi-seq and Pool-seq data without genotyping error.
127 We used established tools for Indi-seq data, and developed a suite of tools for Pool-seq data.
128 GPAS was performed on all the populations with 384 individuals per population for Indi-seq
129 simulating four 96-well sample plates used in high-throughput molecular biology workflows; and
130 5 pools per population for Pool-seq, where each pool consists of 100 individuals. This
131 corresponds to a high power design that was shown to be optimal to capture QTL association
132 (Fournier-Level et al., 2017). GPAS models were trained within each population sampled and
133 cross-validated on all other populations to assess prediction accuracies.

134

135 Allele effects were estimated using 6 Indi-seq-based GPAS (Indi-GPAS) and 3 Pool-seq-based
136 GPAS (Pool-GPAS) modelling frameworks. Efficient mixed-model association expedited model
137 (EMMAX) (Kang et al., 2010), genome-wide complex trait analysis (GCTA) (Jiang et al., 2019),
138 and genome-wide efficient mixed-model analysis (GEMMA) (Zhou & Stephens, 2012) together
139 with GCTA-derived sparse genetic relationship matrix (GRM; off diagonals <0.05 were set to
140 zero) (Jiang et al., 2019; Yang et al., 2010; Zaitlen et al., 2013) and GEMMA-derived
141 standardised relatedness matrix (STD) (Zhou & Stephens, 2012) were used to build the Indi-
142 GPAS models. Genome-wide estimation of additive effects based on trait quantile distribution
143 from Pool-seq data (GWA α) (Fournier-Level et al., 2017), and linear mixed models (LMM)
144 were used to build the Pool-GPAS models, with random effect variance determined by F_{ST}
145 derived using Hivert's (Hivert et al., 2018) or Weir and Cockerham's method (Weir & Cockerham,
146 1984), and variance components estimated using restricted maximum likelihood (REML).

147

148 Phenotype predictions were made using polygenic scores, i.e. the sum of the products of
149 estimated allele effects and allele dosages or allele frequencies. For the Indi-GPAS models and
150 GWAlpha, this involved a two-step approach. For each training set, the polygenic scores of the
151 training set (s_{train}) were calculated as:

$$152 \quad s_{train} = X_{train} \beta,$$

153 where X_{train} is the allele dosage or allele frequency data of the training set, and β are the
154 single-SNP effect estimates. The polygenic scores and actual phenotype values have a linear
155 relationship (Figure S1; mean $R^2_{adjusted}=0.97\pm0.0031$ at 1,000 individuals per population for Indi-
156 seq and mean $R^2_{adjusted}=0.99\pm0.0006$ at 5 pools per population for Pool-seq) as expected under
157 the additive model used to simulate the phenotypes. These polygenic scores were regressed
158 against the actual phenotype values of the training set (y_{train}),

$$159 \quad y_{train} = \alpha_0 + \alpha_1 s_{train},$$

160 where α_0 is the intercept, and α_1 is the slope. The polygenic scores of the validation set,
161 $s_{valid} = X_{valid} \beta$, were transformed into the predicted phenotype values ($y_{predicted}$) using

$$162 \quad y_{predicted} = \alpha_0 + \alpha_1 s_{valid}.$$

163

164 For the Pool-GPAS linear mixed models, the predicted phenotypes ($y_{predicted}$) were calculated
165 as:

$$166 \quad y_{predicted} = X_{valid} \beta,$$

167 where X_{valid} is the matrix of allele frequencies of the validation set, and $\hat{\beta}$ is the estimated
168 allelic effects from the GPAS model built using the training set. The trained models were
169 validated on all populations in the landscape.

170

171 GPAS performance was measured using three GWAS metrics, and one phenotype prediction
172 metric. The GWAS metrics were:

- 173 1. area under the receiver operating curve (AUC) (Fawcett, 2006),
- 174 2. true positive rate (TPR) which was defined as the fraction of causal QTL with a
175 significantly associated SNP within 1 kbp, and
- 176 3. false positive rate (FPR) which was defined as the fraction of the significantly associated
177 SNPs with no causal QTL within 1 kbp, unless it tags a true QTL through a chain of
178 associated SNPs each less than 1kb apart; multiple associated SNPs within 1kbp were
179 counted as one.

180 The family-wise type I error rate was set at $\alpha=0.05$. The metric for phenotype prediction is the
181 root mean square error (RMSE) between actual and predicted phenotype values:

182
$$RMSE = \sqrt{\sum \frac{(y - \hat{y})^2}{n}}$$
,

183 where y is the actual phenotypes, \hat{y} is the predicted phenotypes and n is the number of
184 observations.

185

186 **Sampling strategy optimisation**

187 A total of 405 landscapes were simulated using all combinations of the 4 landscape parameters
188 allowed to vary with 3 levels each and 5 replicates (Table 1). For each landscape, Indi-GPAS

189 and Pool-GPAS experiments were performed for each population independently. This constitutes
190 the intra-population dataset. To simulate the stratified sampling strategy commonly used in
191 ecology (Hoel, 1943; Li et al., 2017; Williams & Brown, 2019), the landscape was divided into
192 equally sized rectangular regions, and the approximately central population was selected from
193 each region. This is illustrated in Figure 1 Panel B. This constitutes the inter-population dataset.
194 AUC and RMSE were averaged across the populations sampled. TPR and FPR were calculated
195 using the cumulative number of true and false positive candidate loci across the populations
196 sampled. AUC was used to measure the accuracy of QTL detection per population, while TPR
197 and FPR were used to measure QTL detection accuracy of multiple populations.

198

199 The single best performing modelling framework was identified for each genotyping scheme
200 (Indi-GPAS and Pool-GPAS) based on AUC and RMSE for independent populations tests using
201 Tukey's honest significant difference (HSD mean comparison) at $\alpha=0.05$.

202

203 How many populations do we need to sample to yield optimal GPAS performance?

204 To determine how many populations to sample to yield optimal GPAS performance, we used the
205 inter-population dataset. We assessed the suitability of the four metrics (i.e. mean AUC, mean
206 RMSE, TPR and FPR) to address this question by visualising their relationships with the number
207 of populations sampled. Additionally, we compared the expected performance of Indi-GPAS and
208 Pool-GPAS under the same sequencing capacity constraint. The Indi-GPAS experiments we
209 simulated included 384 individuals per population, while Pool-GPAS included only 5 pools per
210 population. Assuming a 5X sequencing depth per individual for Indi-seq (Brouard et al., 2017)
211 and the recommended 50X depth per pool for Pool-seq (Schlötterer et al., 2014), these equate

212 to a sequencing depth of 1,920X per base per population for Indi-seq and only 250X for Pool-
213 seq. This means that for the sequencing capacity required to characterise one population
214 through Indi-seq, approximately 7 populations ($\lfloor 1920/250 \rfloor$) could be characterised through
215 Pool-seq.

216

217 Under which landscape-specific circumstances should we use Indi-seq or Pool-seq?

218 The second main question we addressed was which landscape-specific circumstances warrant
219 Indi-GPAS or Pool-GPAS? Specifically, if we were to perform GPAS on one population, which
220 sequencing strategy (Indi-seq or Pool-seq) is better, and how does the optimal choice vary with
221 the polygenicity of the trait, selection intensity, and gene flow? The intra-population dataset was
222 used together with AUC and RMSE as the GPAS performance metrics.

223

224 Which populations to select under different landscape scenarios?

225 To determine which populations to select to best capture the genetic basis of a trait and yield
226 accurate trait predictions, we used AUC and RMSE as the GPAS metrics and the intra-
227 population dataset to test the effect of the three causal allele diffusion gradients. The
228 populations were classified into 10 groups, where each group represents a row perpendicular to
229 the causal allele diffusion gradient. The top row refers to populations 1 to 10, the second row to
230 populations 11 to 20, and so on. The general trends and landscape parameter-specific trends in
231 GPAS performance across the landscape were visualised using violin plots and means
232 compared using Tukey's HSD ($\alpha=0.05$). Linear mixed models fitted linear and quadratic
233 relationships (using second degree polynomial fit) between GPAS performance and the row

234 groups. The row group was treated as a numeric variable, and nested within each level of the
235 parameters: number of QTL, selection intensity, migration rate, and GPAS model.

236

237 **Implementation**

238 The landscapes were simulated using quantiNemo2 (Neuenschwander et al., 2018). The
239 genome and QTL information were simulated in R (R Core Team, 2018). The quantiNemo
240 outputs were parsed using R and Julia (Nardelli et al., 2018). GEMMA (Zhou & Stephens, 2012),
241 EMMAX (Kang et al., 2010), GCTA (Jiang et al., 2019), and Plink (Purcell et al., 2007) were used
242 for Indi-GPAS. [GWAAlpha.jl](#) was used for Pool-GPAS. The R package [violinplotter](#) was used to
243 generate violin plots with HSD mean comparison grouping. The GNU shell (Free Software
244 Foundation, 2016), Spartan (Lafayette & Wiebelt, 2017), Slurm (Yoo et al., 2003), and GNU
245 parallel (Tange, 2011) were used extensively. The workflow is available in the github repository:
246 <https://github.com/jeffersonfparil/GPAS-landscape-simulation.git>.

247

248 **Results**

249 **GPAS model representatives and the relationships of GPAS performance with** 250 **landscape and sampling parameters**

251 GEMMA (STD) and GWAAlpha showed the best GPAS performances, with >79% AUC and <5.9%
252 RMSE (Table S1). Therefore, these two frameworks were selected as the representatives of
253 Indi-GPAS and Pool-GPAS models, respectively. Overall, Indi-GPAS performed better than Pool-
254 GPAS.

255

256 Factors increasing statistical power to identify causal loci through GPAS included a lower
257 number of QTL controlling the trait, more intense selection, higher migration among populations,
258 and more populations sampled (Figure S2). Accuracy in phenotype predictions improved as the
259 number of QTL controlling the trait increases, as selection intensity decreases, and as migration
260 rate increases (Figure S3). Accuracy was unaffected by increasing the number of populations
261 sampled since each model was trained independently for each population. In addition, power
262 and accuracy are high when QTL diffuses across the landscape uniformly.

263

264 **How many populations do we need to sample for optimal GPAS performance?**

265 **And when should we use Indi-seq or Pool-seq?**

266 TPR and FPR increase logarithmically as the number of populations sampled increases (Figure
267 2), so there is no optimum based on these metrics.

268

269 Indi-GPAS achieves greater power than Pool-GPAS at the cost of a higher false positive rate
270 (Figure 2). However, Pool-GPAS can outperform Indi-GPAS under the assumptions detailed in
271 the materials and methods section, where for every population characterised with Indi-seq,
272 approximately 7 populations can be characterised with Pool-seq. Under this 1:7 ratio, Indi-GPAS
273 on 10 populations yield an average TPR of 0.388 and FPR of 0.0150; for the same sequencing
274 capacity Pool-GPAS can be performed on 70 populations, yielding an average TPR of 0.418 and
275 FPR of 0.0115. We explored a range of ratios deviating from this 1:7 ratio. This is because the
276 5X depth requirement for variant calling in Indi-seq and 50X depth for allele frequency estimation
277 in Pool-seq depend on the species of interest and the resources available. Lower ratios, e.g. 1:8
278 to 1:10, mean even more populations can be characterised with Pool-seq for every population

279 characterised with Indi-seq. Using our simulated data to explore various ratios, we find that there
280 exists a range where Pool-GPAS can outperform Indi-GPAS, i.e. TPR is higher and FPR is lower
281 for Pool-GPAS than Indi-GPAS (Figure 3). This shows that characterising more of the landscape
282 at low resolution can be better than characterising a small portion of the landscape at high
283 resolution.

284

285 If we were to perform GPAS on one population, Indi-GPAS is better than Pool-GPAS. However in
286 cases where selection intensity is high (i.e. 0.90 to 0.95) or migration rate is high (i.e. 0.01)
287 Pool-GPAS performance is not significantly different from Indi-GPAS in terms of prediction
288 accuracy (Figure 4).

289

290 **Which populations to select under different landscape scenarios?**

291 GPAS performance is maximised in populations with high genetic variability which at the
292 landscape level, means sampled close to the place of origin of the causal allele (Figure 5). This
293 area of high genetic variability is characterised by intermediate causal allele frequencies which
294 translate into populations with high phenotypic variability. In the absence of a causal allele
295 diffusion gradient (i.e. uniform causal allele distribution), no row seems to be optimal for
296 sampling, except for some slightly better performance from populations in the middle rows.
297 Under unidirectional gradient (i.e. causal alleles originated from the top row and diffused
298 downwards hence a single diffusion front) and in terms of QTL detection accuracy, sampling the
299 populations from the top row is optimal; however, in terms of prediction accuracy, the
300 populations in the middle rows appear to be better. Under bidirectional gradient (i.e. causal
301 alleles originated from the top and bottom rows hence two diffusion fronts) both QTL detection

302 and prediction accuracies are optimal in the populations from the top and bottom rows. These
303 trends across the landscape coincide with the trends in the mean number of polymorphic QTL
304 per population and causal allele frequencies.

305

306 In the presence of causal allele diffusion gradients, the relationships between QTL detection or
307 prediction accuracies and the sampling location (defined as rows perpendicular to the diffusion
308 gradient) appear to be quadratic, except for QTL detection accuracy under unidirectional causal
309 allele diffusion, for which the relationship is linear (Figure 5). In terms of GWAS accuracy as
310 measured by AUC, sampling near the diffusion fronts becomes less important (i.e. slope under
311 unidirectional gradient and curvature under bidirectional gradient are reduced) as the number of
312 QTL increases, as selection intensity decreases, and as migration rate increases (Figure 6
313 columns 1-3). In addition, sampling near the diffusion fronts is more important for Pool-GPAS
314 than Indi-GPAS (Figure 6 column 4), in other words, power diminishes quicker for Pool-GPAS
315 than Indi-GPAS as we move away from areas of high diversity.

316

317 In terms of prediction accuracy as measured by RMSE, the degree to which the middle rows (i.e.
318 areas of high genetic and phenotypic variability) are the optimal sampling locations under
319 unidirectional diffusion decreases (i.e. curvature becomes less severe) as the number of QTL
320 increases, as selection intensity decreases, and as migration rate increases (Figure 7 top
321 graphs). Also, sampling from the middle rows under unidirectional diffusion is slightly more
322 important for Indi-GPAS than Pool-GPAS. On the other hand, the degree to which the top and
323 bottom rows are optimal under bidirectional diffusion decreases (i.e. curvature becomes less
324 severe) as the number of QTL, selection intensity, and migration rate increase (Figure 7 bottom

325 graphs). Also, sampling from the top and bottom rows under bidirectional diffusion is more
326 important for Pool-GPAS than Indi-GPAS, in other words, similar to that of power, accuracy
327 diminishes quicker for Pool-GPAS than Indi-GPAS as we move away from areas of high
328 diversity.

329

330 These trends in GPAS performance across the landscape under variable parameter levels
331 correlate with the trends in genetic variability (expressed in terms of causal allele frequency, i.e.
332 frequencies closer to 0.5 indicates higher diversity) across the landscape (Figures S4 to S9).
333 The opposite trends observed between causal allele diffusion gradients for RMSE as selection
334 intensity increases is explained by the shift of the optimal row. At low selection intensity under
335 unidirectional causal allele diffusion, the relationship between RMSE and the row group is linear,
336 i.e. sampling near the diffusion front is better than sampling the middle rows (Figure S5). At high
337 selection intensity under bidirectional causal allele diffusion, the rows in between the middle and
338 top rows, as well as in between the middle and bottom rows become the optima (Figure S8).

339

340 **Discussion**

341 **GPAS in ecology and evolution**

342 GPAS has the potential to expand genomic studies in ecology and evolution beyond
343 environment association and niche modelling (Dormann et al., 2012; Exposito-Alonso et al.,
344 2018; Fournier-Level et al., 2011). By focusing on functional traits, GWAS can identify QTL
345 controlling fitness and other ecologically important traits in natural populations. GP exploits the
346 same modelling framework as GWAS to predict phenotype values for the rapid monitoring of
347 species adaptation to existing or changing environmental conditions. The predicted

348 environmental range of individuals using genome-environment associations (Manel et al., 2018)
349 can be complemented by the phenotype predictions of GPAS. This can be transformational for
350 the way we monitor invasive species or assess the adaptive potential of endangered species.

351

352 Our results complement previous research on sampling optimisation in ecology and evolution.
353 We specifically focused on providing recommendations on the optimal sampling strategy to
354 maximise the power to detect QTL and the accuracy of quantitative phenotype prediction in
355 natural populations. We stress the importance of capturing sufficient representation of the
356 genetic variability present over the landscape by sampling populations from areas of high
357 genetic diversity. On a per population basis or if only one population were to be sampled, we
358 recommend using Indi-seq over Pool-seq. We have not here considered phenotyping costs, but
359 higher costs would increase the attractiveness of Indi-seq to maximise information per unit cost.
360 However, similar to a meta analysis of several landscape genomics studies (Santos & Gaiotto,
361 2020) we demonstrate the value of Pool-seq in maximising the number of populations that can
362 be analysed without compromising power. This is especially true if the aim is to predict
363 phenotypes of some future populations for the rapid and timely monitoring of invasive and
364 threatened species.

365

366 Indi-seq provides high-resolution genomic information for a population, but comes at a high cost.
367 A given genomic region needs to be sequenced at least 5 times for each individual to yield
368 accurate basecalling information (Brouard et al., 2017), and many individuals are required to
369 accurately represent a population. This is only resource-effective when the individuals are part of
370 an association panel and the genomic information can be leveraged for several research

371 projects (Robin et al., 2019). On the other hand, Pool-seq generates low-resolution genomic
372 information on a population that is cost-effective while maintaining high power. Hundreds of
373 individuals can be pooled to yield accurate allele frequency data (Schlötterer et al., 2014). This
374 means that a few pools consisting of hundreds of individuals each can represent a population
375 better than a few individual sequences. As expected, Pool-seq is more widely used than Indi-seq
376 in ecological and evolutionary studies because the focus is generally on populations rather than
377 individuals, and because of its cost-effectiveness (Futschik & Schlötterer, 2010). In contrast,
378 Cutler and Jensen (2010) concluded that Indi-seq should be preferred over Pool-seq for many
379 applications due to the loss of haplotype and LD information. They focused on applications in
380 human and model organisms, whereas Pool-seq has its highest impact for high-throughput data
381 acquisition in non-model species of critical ecological and economical importance.

382

383 The GPAS models used in this study are representative of quantitative genetics modelling
384 frameworks utilising Indi-seq and Pool-seq genomic data. GEMMA using the standardised
385 relatedness matrix is routinely used for association studies in crops (Begum et al., 2015; Wang
386 et al., 2016; Xiao et al., 2017), livestock (Li et al., 2019; Smith et al., 2019; Wu et al., 2019), and
387 humans (Charng et al., 2020; Fatumo et al., 2019). GWAlpha is a parametric method for
388 estimating additive allelic effects from Pool-seq data that goes beyond the use of just two
389 extreme pools. In this study we have shown that allelic effects estimated using GWAlpha can be
390 used to predict trait values as accurately as Indi-GPAS. In ecological and evolutionary context,
391 Indi-GPAS is performed mostly on model species, e.g. *Arabidopsis thaliana* and *Drosophila*
392 *melanogaster*, because of the wealth of individual genomic information readily available (1001
393 Genomes Consortium, 2016; Exposito-Alonso et al., 2018; Flatt, 2020; Mackay et al., 2012). The

394 cost-effectiveness of Pool-seq can help close the gap in the application of these powerful
395 statistical frameworks between model and non-model species. Hence, Pool-GPAS with
396 GWAlpha can bring a powerful and cost-effective framework to ecology and evolution for the
397 identification of the genetic basis of quantitative traits and the prediction of trait values for the
398 rapid monitoring of species adaptation.

399

400 **GPAS performance as affected by trait polygenicity and landscape properties**

401 QTL detection and phenotype prediction accuracies can have similar or contrasting responses to
402 varying genetic architectures and landscape properties. QTL detection power increases as the
403 contribution of each QTL to the trait increases and as the frequency of QTL alleles is balanced
404 (ie. close to 0.5). On the other hand, prediction accuracy increases as the total additive genetic
405 variance increases. Allele frequencies and additive genetic variance vary in response to
406 evolutionary forces, e.g. selection intensity and migration rate. Some prior knowledge of the
407 polygenicity of the trait and the spatial heterogeneity of selection intensity and gene flow is
408 valuable for identifying the optimal locations for population sampling.

409

410 There is less power to detect QTL but higher prediction accuracy in highly polygenic traits than
411 traits controlled by fewer loci. Increasing the number of loci controlling the trait reduces the
412 selection pressure acting on each locus (Walsh & Lynch, 2018). This decreases the power to
413 detect QTL since the individual contribution of each QTL decreases as more loci control the trait
414 (Wang & Xu, 2019). This in turn reduces the proportion of polymorphic QTL within populations: if
415 the majority of the QTL have small effects, they have a higher chance of getting lost due to drift
416 than QTL with large effects. On the other hand, prediction accuracy increases since the rate at

417 which genetic variance decreases due to directional selection is reduced as the number of QTL
418 increases. Genetic variance should eventually become zero under constant stabilising or
419 directional selection, but the rate of this reduction becomes slower with an increased number of
420 loci controlling the trait (Crow & Kimura, 1970). Hence, GWAS and GP complement each other
421 to achieve high QTL detection accuracy or high prediction accuracy for quantitative traits
422 controlled by any number of loci.

423

424 There is higher power to detect QTL but lower prediction accuracy in populations under intense
425 selection. Increasing the selection intensity increases QTL detection power, since the
426 contribution of individual QTL becomes greater in each population (Wang & Xu, 2019) and less
427 QTL alleles are lost due to drift. However, the predictive ability will be reduced by the Bulmer
428 effect (Bulmer, 1971), where covariance between loci (partially explained by linkage
429 disequilibrium (Walsh & Lynch, 2018)) is reduced after selection. Increasing selection intensity
430 magnifies this reduction resulting in diminished additive genetic variance and less predictive
431 models. This further solidifies the complementary nature of GWAS and GP and the utility of
432 performing both with GPAS.

433

434 There is more power to detect QTL and greater prediction accuracy in populations experiencing
435 high migration than in reproductively isolated ones. Increasing migration rate decreases
436 differentiation between populations allowing for more causal alleles to be shared, resulting in
437 higher power and more accurate predictions. This is expected to reduce the contribution of each
438 QTL since the number of QTL per population increases thereby decreasing power (Griswold,
439 2006; Wang & Xu, 2019). However, our results suggest the opposite: power increases as

440 migration increases. This is because the total number of loci controlling the trait does not
441 increase per se, only the proportion of the polymorphic QTL per population does, which leads to
442 higher variance for these QTL per population. Increasing the additive genetic variance in each
443 population (Liu et al., 2020) also results in higher prediction accuracy.

444

445 **Sampling strategy for GPAS in ecology and evolution**

446 The results of this simulation study emphasise the need to sample as many populations as
447 possible from regions of high genetic diversity. The power to detect QTL is maximised if all the
448 populations in the landscape were included in the study. This is possible for highly endangered
449 species with a small number of populations in the wild. However this is not feasible for species
450 with a healthier number of populations. The best populations to sample are located in areas of
451 high genetic diversity which manifests as areas with high trait variability where the causal alleles
452 are at intermediate frequencies.

453

454 Our results show a diminishing return in terms of GPAS power when sampling an increasing
455 number of populations. This is consistent with a previous study on sampling strategy
456 optimisation which found that sampling an intermediate number of sites can perform as well as
457 maximising the number of sites sampled (Selmoni et al., 2020). This study only considered Indi-
458 seq and tested different sample sizes per population, and our approach is comparable because
459 using Indi-seq equates to a high-resolution characterisation of the landscape and Pool-seq to a
460 low-resolution one. Our analysis extends this result further because it is independent of the
461 number of individuals sampled per population. The cost-effectiveness of Pool-seq allows for
462 more populations to be sampled and included in the study than Indi-seq.

463

464 The number of individuals per population selected for our Indi-GPAS simulations (384
465 individuals) exceeds the sample size of most ecological studies (e.g. 100-200 individual samples
466 per population in birds (Hansson et al., 2018; Perrier et al., 2018), <100 samples per population
467 in trees (Cappa et al., 2013; Holliday et al., 2010), ~100 samples per population in mammals
468 (Johnston et al., 2011; Pallares et al., 2014), and <20 samples per population in fish (Willing et
469 al., 2010)). Thus for most experiments, the power of Indi-GPAS is expected to be lower than in
470 our simulations. On the contrary, the power of Pool-GPAS is expected to remain the same since
471 five pools per population was found to be optimal (Fournier-Level et al., 2017) and each pool can
472 include a non-limiting number of individuals. The sequencing capacity required for Indi-seq is
473 always higher than Pool-seq and more populations can be characterised with Pool-seq than Indi-
474 seq under the same budgetary constraints (Schlötterer et al., 2014). Therefore, the range of the
475 number of populations sampled where Pool-GPAS outperforms Indi-GPAS is likely to be even
476 broader than reported here, as long as the genomic characterisation approach yields accurate
477 genomic data.

478

479 We have shown that sampling from genetically diverse populations maximises GPAS
480 performance. Capturing greater genetic diversity was shown to increase the power to detect
481 causal loci (Alqudah et al., 2020; Rosenberg et al., 2010; Wojcik et al., 2019). Similarly,
482 populations which represent the overall diversity found in the landscape or are similar to the
483 validation populations, improve prediction accuracies (Akdemir & Isidro-Sánchez, 2019; Asoro et
484 al., 2011; Edwards et al., 2019). Populations with high genetic diversity were found along the
485 diffusion fronts, i.e. the areas where the causal alleles migrate from their site of origin into the

486 neighbouring populations. The rate at which GPAS performance decreases as we sample farther
487 away from the diffusion fronts correlates with the decrease in genetic diversity at the causal loci.
488 In the absence of prior genomic information, the areas of high genetic diversity coincide with
489 regions of high phenotypic diversity. Gaining prior information on the location of these areas of
490 high genetic diversity and causal allele diffusion fronts or more broadly the landscape of
491 adaptive genetic diversity (Eckert & Dyer, 2012) is key to an optimal sampling strategy.

492

493 When the causal allele diffusion gradient is unknown and a uniform causal allele distribution is
494 assumed there is a small advantage in choosing populations in the middle of the landscape. This
495 can be explained by the absorbing boundaries used in the migration model which simulates a
496 restricted range whereby alleles going beyond the border are lost. In the context of a species
497 distributed over a restricted range, alleles have a higher probability of getting lost in border
498 populations than in the populations in the middle of the range. The non-linear relationship
499 between the RMSE and the distance from the diffusion front under unidirectional diffusion
500 gradient also highlights this border effect. Populations in the middle of the distribution range
501 have a similar number of polymorphic causal loci as the populations closer to the diffusion front.
502 This phenomenon reflects what happens in fringe populations where migration regularly occurs
503 beyond the suitable environmental niche of the species and the migrants fail to survive (Sexton
504 et al., 2009). Hence, in the absence of prior information on the location of high genetic diversity,
505 we do not recommend sampling from these fringe or border populations.

506

507

508

509 **Conclusion**

510 Genome-wide association studies and genomic prediction (GPAS) are poised to complement
511 existing methodologies in ecology in evolution. GPAS provides powerful tools to dissect the
512 genetic basis of ecologically important quantitative traits including fitness and to rapidly monitor
513 natural populations including invasive and threatened species. Understanding how the number
514 of population samples and the different landscape properties affect the QTL detection power and
515 phenotype prediction accuracies is integral to planning population collections for GPAS
516 experiments. We recommend sampling as many populations as possible from areas of high
517 genetic diversity. We also recommend Pool-seq whenever Indi-seq is too costly; since sampling
518 more populations at the cost of lower resolution can be better than characterising a small
519 number of populations at high resolution. The complementary nature of GWAS and GP allows
520 good QTL detection power or prediction accuracy under low to high trait polygenicity and
521 selection intensity. In the absence of prior information on the areas of high genetic diversity, we
522 recommend against sampling populations at the border of the species' range.

523

524

525 **Acknowledgments**

526 The authors wish to thank Uli Felzmann from IT services, Faculty of Science, The University of
527 Melbourne for his outstanding support. We acknowledge the extensive use of the Spartan High
528 Performance Computing and the Melbourne Research Cloud systems. Part of this work was
529 supported through the Computational Biology Research Initiative Seed Fund awarded to AF-L.
530

531 **Data accessibility**

532 Codes to reproduce the simulation data and the subsequent analysis are publicly available on
533 github: <https://github.com/jeffersonparil/GPAS-landscape-simulation>.
534

535 **Author Contributions**

536 JFP, DJB and AFL designed the study. JFP analysed the data. JFP and AFL wrote the
537 manuscript with input from DJB.

538 **References**

539 1001 Genomes Consortium, J., 1001 Genomes Consortium. (2016). 1,135 Genomes Reveal the
540 Global Pattern of Polymorphism in *Arabidopsis thaliana*. *Cell*, *166*(2), 481–491. doi:
541 10.1016/j.cell.2016.05.063

542 Akdemir, D., & Isidro-Sánchez, J. (2019). Design of training populations for selective
543 phenotyping in genomic prediction. *Scientific Reports*, *9*(1), 1446. doi: 10.1038/s41598-
544 018-38081-6

545 Alqudah, A. M., Sallam, A., Stephen Baenziger, P., & Börner, A. (2020). GWAS: Fast-forwarding
546 gene identification and characterization in temperate Cereals: lessons from Barley – A
547 review. *Journal of Advanced Research*, *22*, 119–135. doi: 10.1016/j.jare.2019.10.013

548 Asoro, F. G., Newell, M. A., Beavis, W. D., Scott, M. P., & Jannink, J.-L. (2011). Accuracy and
549 Training Population Design for Genomic Selection on Quantitative Traits in Elite North
550 American Oats. *The Plant Genome*, *4*(2), 132–144. doi:
551 10.3835/plantgenome2011.02.0007

552 Baird, N. A., Etter, P. D., Atwood, T. S., Currey, M. C., Shiver, A. L., Lewis, Z. A., ... Johnson, E.
553 A. (2008). Rapid SNP Discovery and Genetic Mapping Using Sequenced RAD Markers.
554 *PLoS ONE*, *3*(10), e3376. doi: 10.1371/journal.pone.0003376

555 Bastide, H., Betancourt, A., Nolte, V., Tobler, R., Stöbe, P., Futschik, A., & Schlotterer, C. (2013).
556 A Genome-Wide, Fine-Scale Map of Natural Pigmentation Variation in *Drosophila*
557 *melanogaster*. *PLoS Genetics*, *9*(6), e1003534. doi: 10.1371/journal.pgen.1003534

558 Begum, H., Spindel, J. E., Lalusin, A., Borromeo, T., Gregorio, G., Hernandez, J., ... McCouch,
559 S. R. (2015). Genome-Wide Association Mapping for Yield and Other Agronomic Traits in
560 an Elite Breeding Population of Tropical Rice (*Oryza sativa*). *PLoS ONE*, *10*(3). doi:
561 10.1371/journal.pone.0119873

562 Beissinger, T. M., Hirsch, C. N., Vaillancourt, B., Deshpande, S., Barry, K., Buell, C. R., ... de
563 Leon, N. (2014). A genome-wide scan for evidence of selection in a maize population
564 under long-term artificial selection for ear number. *Genetics*, *196*(3), 829–40. doi:
565 10.1534/genetics.113.160655

566 Bélanger, S., Esteves, P., Clermont, I., Jean, M., & Belzile, F. (2016). Genotyping-by-Sequencing
567 on Pooled Samples and its Use in Measuring Segregation Bias during the Course of
568 Androgenesis in Barley. *The Plant Genome*, *9*(1), 0. doi:
569 10.3835/plantgenome2014.10.0073

570 Boitard, S., Schlotterer, C., Nolte, V., Pandey, R. V., & Futschik, A. (2012). Detecting Selective
571 Sweeps from Pooled Next-Generation Sequencing Samples. *Molecular Biology and*
572 *Evolution*, *29*(9), 2177–2186. doi: 10.1093/molbev/mss090

573 Brouard, J.-S., Boyle, B., Ibeagha-Awemu, E. M., & Bissonnette, N. (2017). Low-depth

584 genotyping-by-sequencing (GBS) in a bovine population: strategies to maximize the
585 selection of high quality genotypes and the accuracy of imputation. *BMC Genetics*, 18.
586 doi: 10.1186/s12863-017-0501-y
587

588 Bulmer, M. G. (1971). The Effect of Selection on Genetic Variability. *The American Naturalist*.
589 Retrieved from <https://www.journals.uchicago.edu/doi/10.1086/282718>
590

591 Cappa, E. P., El-Kassaby, Y. A., Garcia, M. N., Acuña, C., Borralho, N. M. G., Grattapaglia, D., &
592 Poltri, S. N. M. (2013). Impacts of Population Structure and Analytical Models in
593 Genome-Wide Association Studies of Complex Traits in Forest Trees: A Case Study in
594 Eucalyptus globulus. *PLOS ONE*, 8(11), e81267. doi: 10.1371/journal.pone.0081267
595

596 Charng, J., Simcoe, M., Sanfilippo, P. G., Allingham, R. R., Hewitt, A. W., Hammond, C. J., ...
597 Yazar, S. (2020). Age-dependent regional retinal nerve fibre changes in SIX1/SIX6
598 polymorphism. *Scientific Reports*, 10. doi: 10.1038/s41598-020-69524-8
599

600 Cheng, C., White, B. J., Kamdem, C., Mockaitis, K., Costantini, C., Hahn, M. W., & Besansky, N.
601 J. (2012). Ecological genomics of anopheles gambiae along a latitudinal cline: A
602 population-resequencing approach. *Genetics*, 190(4), 1417–1432. doi:
603 10.1534/genetics.111.137794
604

605 Crow, J. F., & Kimura, M. (1970). *An Introduction to Population Genetics Theory*. doi:
606 10.2307/1529706
607

608 Cutler, D. J., & Jensen, J. D. (2010). To pool, or not to pool? *Genetics*, 186(1), 41–3. doi:
609 10.1534/genetics.110.121012
610

611 de Roos, A. P. W., Hayes, B. J., & Goddard, M. E. (2009). Reliability of genomic predictions
612 across multiple populations. *Genetics*, 183(4), 1545–53. doi:
613 10.1534/genetics.109.104935
614

615 Dormann, C. F., Schymanski, S. J., Cabral, J., Chuine, I., Graham, C., Hartig, F., ... Singer, A.
616 (2012). Correlation and process in species distribution models: bridging a dichotomy.
617 *Journal of Biogeography*, 39(12), 2119–2131. doi: 10.1111/j.1365-2699.2011.02659.x
618

619 Eckert, A. J., & Dyer, R. J. (2012). Defining the landscape of adaptive genetic diversity.
620 *Molecular Ecology*, 21(12), 2836–2838. doi: 10.1111/j.1365-294X.2012.05615.x
621

622 Edwards, S. M., Buntjer, J. B., Jackson, R., Bentley, A. R., Lage, J., Byrne, E., ... Hickey, J. M.
623 (2019). The effects of training population design on genomic prediction accuracy in
624 wheat. *Theoretical and Applied Genetics*, 132(7), 1943–1952. doi: 10.1007/s00122-019-
625 03327-y
626

627 Exposito-Alonso, M., Vasseur, F., Ding, W., Wang, G., Burbano, H. A., & Weigel, D. (2018).
628 Genomic basis and evolutionary potential for extreme drought adaptation in *Arabidopsis*
629 *thaliana*. *Nature Ecology & Evolution*, 2(2), 352–358. doi: 10.1038/s41559-017-0423-0

630
631 Fariello, M. I., Boitard, S., Mercier, S., Robelin, D., Faraut, T., Arnould, C., ... SanCristobal, M.
632 (2017). Accounting for linkage disequilibrium in genome scans for selection without
633 individual genotypes: The local score approach. *Molecular Ecology*, 26(14), 3700–3714.
634 doi: 10.1111/mec.14141

635
636 Fatumo, S., Carstensen, T., Nashiru, O., Gurdasani, D., Sandhu, M., & Kaleebu, P. (2019).
637 Complimentary Methods for Multivariate Genome-Wide Association Study Identify New
638 Susceptibility Genes for Blood Cell Traits. *Frontiers in Genetics*, 10. doi:
639 10.3389/fgene.2019.00334

640
641 Fawcett, T. (2006). An introduction to ROC analysis. *Pattern Recognition Letters*, 27(8), 861–
642 874. doi: 10.1016/j.patrec.2005.10.010

643
644 Flatt, T. (2020). Life-History Evolution and the Genetics of Fitness Components in *Drosophila*
645 *melanogaster*. *Genetics*, 214(1), 3–48. doi: 10.1534/genetics.119.300160

646
647 Fournier-Level, A., Korte, A., Cooper, M. D., Nordborg, M., Schmitt, J., & Wilczek, A. M. (2011). A
648 Map of Local Adaptation in *Arabidopsis thaliana*. *Science*, 334(6052), 86–89. doi:
649 10.1126/science.1209271

650
651 Fournier-Level, Alexandre, Robin, C., & Balding, D. J. (2017). GWAlpha: Genome-wide
652 estimation of additive effects (alpha) based on trait quantile distribution from pool-
653 sequencing experiments. *Bioinformatics*. doi: 10.1093/bioinformatics/btw805

654
655 Fracassetti, M., Griffin, P. C., & Willi, Y. (2015). Validation of Pooled Whole-Genome Re-
656 Sequencing in *Arabidopsis lyrata*. *PloS One*, 10(10), e0140462. doi:
657 10.1371/journal.pone.0140462

658
659 Free Software Foundation. (2016). *GNU bash*. Retrieved from
660 <https://www.gnu.org/software/bash/>

661
662 Futschik, A., & Schlötterer, C. (2010). The next generation of molecular markers from massively
663 parallel sequencing of pooled DNA samples. *Genetics*, 186(1), 207–18. doi:
664 10.1534/genetics.110.114397

665
666 Gautier, M., Foucaud, J., Gharbi, K., Cézard, T., Galan, M., Loiseau, A., ... Estoup, A. (2013).
667 Estimation of population allele frequencies from next-generation sequencing data: pool-
668 versus individual-based genotyping. *Molecular Ecology*, 22(14), 3766–3779. doi: 10.1111/
669 mec.12360

670
671 Gondro, C., van der Werf, J., & Hayes, B. (Eds.). (2013). *Genome-wide association studies and*
672 *genomic prediction* (1st ed.). Humana Press. doi: 10.1007/978-1-62703-447-0_20

673
674 Griswold, C. K. (2006). Gene flow's effect on the genetic architecture of a local adaptation and
675 its consequences for QTL analyses. *Heredity*, 96(6), 445–453. doi:

676 10.1038/sj.hdy.6800822
677
678 Guo, X., Cericola, F., Fè, D., Pedersen, M. G., Lenk, I., Jensen, C. S., ... Janss, L. L. (2018).
679 Genomic Prediction in Tetraploid Ryegrass Using Allele Frequencies Based on
680 Genotyping by Sequencing. *Frontiers in Plant Science*, 9, 1165. doi:
681 10.3389/fpls.2018.01165
682
683 Hansson, B., Sigeman, H., Stervander, M., Tarka, M., Ponnikas, S., Strandh, M., ... Hasselquist,
684 D. (2018). Contrasting results from GWAS and QTL mapping on wing length in great
685 reed warblers. *Molecular Ecology Resources*, 18(4), 867–876. doi: 10.1111/1755-
686 0998.12785
687
688 Hivert, V., Leblois, R., Petit, E. J., Gautier, M., & Vitalis, R. (2018). Measuring Genetic
689 Differentiation from Pool-seq Data. *Genetics*, 210(1), 315–330. doi:
690 10.1534/genetics.118.300900
691
692 Hoel, P. (1943). The Accuracy of Sampling Methods in Ecology on JSTOR. *The Annals of*
693 *Mathematical Statistics*, 14(3), 289–300.
694
695 Holliday, J. A., Ritland, K., & Aitken, S. N. (2010). Widespread, ecologically relevant genetic
696 markers developed from association mapping of climate-related traits in Sitka spruce
697 (*Picea sitchensis*). *New Phytologist*, 188(2), 501–514. doi: 10.1111/j.1469-
698 8137.2010.03380.x
699
700 Jiang, L., Zheng, Z., Qi, T., Kemper, K. E., Wray, N. R., Visscher, P. M., & Yang, J. (2019). A
701 resource-efficient tool for mixed model association analysis of large-scale data. *Nature*
702 *Genetics*, 51(12), 1749–1755. doi: 10.1038/s41588-019-0530-8
703
704 Johnston, S. E., McEWAN, J. C., Pickering, N. K., Kijas, J. W., Beraldi, D., Pilkington, J. G., ...
705 Slate, J. (2011). Genome-wide association mapping identifies the genetic basis of
706 discrete and quantitative variation in sexual weaponry in a wild sheep population.
707 *Molecular Ecology*, 20(12), 2555–2566. doi: 10.1111/j.1365-294X.2011.05076.x
708
709 Kang, H. M., Sul, J. H., Service, S. K., Zaitlen, N. A., Kong, S., Freimer, N. B., ... Eskin, E.
710 (2010). Variance component model to account for sample structure in genome-wide
711 association studies. *Nature Genetics*, 42(4), 348–354. doi: 10.1038/ng.548
712
713 Knight, J., Saccone, S. F., Zhang, Z., Ballinger, D. G., & Rice, J. P. (2009). A Comparison of
714 Association Statistics between Pooled and Individual Genotypes. *Human Heredity*, 67(4),
715 219–225. doi: 10.1159/000194975
716
717 Lafayette, L., & Wiebelt, B. (2017). Spartan and NEMO: Two HPC-Cloud Hybrid
718 Implementations. *2017 IEEE 13th International Conference on E-Science (e-Science)*,
719 458–459. Auckland: IEEE. doi: 10.1109/eScience.2017.70
720
721 Li, X., Nie, C., Liu, Y., Chen, Y., Lv, X., Wang, L., ... Qu, L. (2019). A genome-wide association

722 study explores the genetic determinism of host resistance to *Salmonella pullorum*
723 infection in chickens. *Genetics, Selection, Evolution: GSE*, 51. doi: 10.1186/s12711-019-
724 0492-4

725
726 Li, Y., Zhang, X.-X., Mao, R.-L., Yang, J., Miao, C.-Y., Li, Z., & Qiu, Y.-X. (2017). Ten Years of
727 Landscape Genomics: Challenges and Opportunities. *Frontiers in Plant Science*, 8,
728 2136. doi: 10.3389/fpls.2017.02136

729
730 Liu, L., Wang, Y., Zhang, D., Chen, Z., Chen, X., Su, Z., & He, X. (2020). The Origin of Additive
731 Genetic Variance Driven by Positive Selection. *Molecular Biology and Evolution*, 37(8),
732 2300–2308. doi: 10.1093/molbev/msaa085

733
734 Long, A. D., & Langley, C. H. (1999). The Power of Association Studies to Detect the
735 Contribution of Candidate Genetic Loci to Variation in Complex Traits. *Genome*
736 *Research*, 9(8), 720–731. doi: 10.1101/gr.9.8.720

737
738 Macgregor, S., Visscher, P. M., & Montgomery, G. (2006). Analysis of pooled DNA samples on
739 high density arrays without prior knowledge of differential hybridization rates. *Nucleic*
740 *Acids Research*, 34(7). doi: 10.1093/nar/gkl136

741
742 Mackay, T. F. C., Richards, S., Stone, E. A., Barbadilla, A., Ayroles, J. F., Zhu, D., ... Gibbs, R. A.
743 (2012). The *Drosophila melanogaster* Genetic Reference Panel. *Nature*, 482(7384), 173–
744 178. doi: 10.1038/nature10811

745
746 Manel, S., Andrello, M., Henry, K., Verdelet, D., Darracq, A., Guerin, P.-E., ... Devaux, P. (2018).
747 Predicting genotype environmental range from genome–environment associations.
748 *Molecular Ecology*, 27(13), 2823–2833. doi: 10.1111/mec.14723

749
750 Micheletti, S. J., & Narum, S. R. (2018). Utility of pooled sequencing for association mapping in
751 nonmodel organisms. *Molecular Ecology Resources*, 18(4), 825–837. doi: 10.1111/1755-
752 0998.12784

753
754 Neuenschwander, S., Michaud, F., Goudet, J., & Stegle, O. (2018). quantiNemo 2: a swiss knife
755 to simulate complex demographic and genetic scenarios, forward and backward in time.
756 *Bioinformatics*. doi: 10.1093/bioinformatics/bty737

757
758 Nielsen, E. S., Henriques, R., Toonen, R. J., Knapp, I. S. S., Guo, B., & von der Heyden, S.
759 (2018). Complex signatures of genomic variation of two non-model marine species in a
760 homogeneous environment. *BMC Genomics*, 19(1), 347. doi: 10.1186/s12864-018-4721-
761 y

762
763 Pallares, L. F., Harr, B., Turner, L. M., & Tautz, D. (2014). Use of a natural hybrid zone for
764 genomewide association mapping of craniofacial traits in the house mouse. *Molecular*
765 *Ecology*, 23(23), 5756–5770. doi: 10.1111/mec.12968

766
767 Perrier, C., Delahaie, B., & Charmantier, A. (2018). Heritability estimates from genomewide

768 relatedness matrices in wild populations: Application to a passerine, using a small
769 sample size. *Molecular Ecology Resources*, 18(4), 838–853. doi: 10.1111/1755-
770 0998.12886

771
772 Purcell, S., Neale, B., Todd-Brown, K., Thomas, L., Ferreira, M. A. R., Bender, D., ... Sham, P. C.
773 (2007). PLINK: A Tool Set for Whole-Genome Association and Population-Based Linkage
774 Analyses. *The American Journal of Human Genetics*, 81(3), 559–575. doi:
775 10.1086/519795

776
777 R Core Team. (2018). *R: A Language and Environment for Statistical Computing*. Vienna,
778 Austria. Retrieved from <https://www.r-project.org/>

779
780 Rellstab, C., Zoller, S., Tedder, A., Gugerli, F., & Fischer, M. C. (2013). Validation of SNP Allele
781 Frequencies Determined by Pooled Next-Generation Sequencing in Natural Populations
782 of a Non-Model Plant Species. *PLoS ONE*, 8(11), e80422. doi:
783 10.1371/journal.pone.0080422

784
785 Richards, F. J. (1959). A flexible growth function for empirical use. *Journal of Experimental*
786 *Botany*, 10(2), 290–301. doi: 10.1093/jxb/10.2.290

787
788 Robin, C., Battlay, P., & Fournier-Level, A. (2019). What can genetic association panels tell us
789 about evolutionary processes in insects? *Current Opinion in Insect Science*, 31, 99–105.
790 doi: 10.1016/j.cois.2018.12.004

791
792 Rosenberg, N. A., Huang, L., Jewett, E. M., Szpiech, Z. A., Jankovic, I., & Boehnke, M. (2010).
793 Genome-wide association studies in diverse populations. *Nature Reviews Genetics*,
794 11(5), 356–366. doi: 10.1038/nrg2760

795
796 Santos, A. S., & Gaiotto, F. A. (2020). Knowledge status and sampling strategies to maximize
797 cost-benefit ratio of studies in landscape genomics of wild plants. *Scientific Reports*,
798 10(1), 1–9. doi: 10.1038/s41598-020-60788-8

799
800 Schlötterer, C., Tobler, R., Kofler, R., & Nolte, V. (2014). Sequencing pools of individuals - mining
801 genome-wide polymorphism data without big funding. *Nature Reviews*, 15, 749–765.

802
803 Selmoni, O., Vajana, E., Guillaume, A., Rochat, E., & Joost, S. (2020). Sampling strategy
804 optimization to increase statistical power in landscape genomics: A simulation-based
805 approach. *Molecular Ecology Resources*, 20(1), 154–169. doi: 10.1111/1755-0998.13095

806
807 Sexton, J. P., McIntyre, P. J., Angert, A. L., & Rice, K. J. (2009). Evolution and Ecology of
808 Species Range Limits. *Annual Review of Ecology, Evolution, and Systematics*, 40(1),
809 415–436. doi: 10.1146/annurev.ecolsys.110308.120317

810
811 Smith, J. L., Wilson, M. L., Nilson, S. M., Rowan, T. N., Oldeschulte, D. L., Schnabel, R. D., ...
812 Seabury, C. M. (2019). Genome-wide association and genotype by environment
813 interactions for growth traits in U.S. Gelbvieh cattle. *BMC Genomics*, 20(1), 926. doi:

814 10.1186/s12864-019-6231-y
815
816 Tange, O. (2011). *GNU Parallel - The Command-Line Power Tool*. The USENIX Magazine.
817
818 Walsh, B., & Lynch, M. (2018). *Evolution and selection of quantitative traits* (1st ed.). Oxford
819 University Press. Retrieved from
820 http://nitro.biosci.arizona.edu/zbook/NewVolume_2/newvol2.html#2B
821
822 Wang, H., Xu, X., Vieira, F. G., Xiao, Y., Li, Z., Wang, J., ... Chu, C. (2016). The Power of
823 Inbreeding: NGS-Based GWAS of Rice Reveals Convergent Evolution during Rice
824 Domestication. *Molecular Plant*, 9(7), 975–985. doi: 10.1016/j.molp.2016.04.018
825
826 Wang, M., & Xu, S. (2019). Statistical power in genome-wide association studies and
827 quantitative trait locus mapping. *Heredity*, 123(3), 287–306. doi: 10.1038/s41437-019-
828 0205-3
829
830 Weir, B. S., & Cockerham, C. C. (1984). Estimating F-Statistics for the Analysis of Population
831 Structure Author (s): B . S . Weir and C . Clark Cockerham Reviewed work (s):
832 Published by : Society for the Study of Evolution Stable URL :
833 <http://www.jstor.org/stable/2408641> . *Evolution*, 38(6), 1358–1370. doi: 128.103.149.52
834
835 Williams, B. K., & Brown, E. D. (2019). Sampling and analysis frameworks for inference in
836 ecology. *Methods in Ecology and Evolution*, 10(11), 1832–1842. doi: 10.1111/2041-
837 210X.13279
838
839 Willing, E.-M., Bentzen, P., Oosterhout, C. V., Hoffmann, M., Cable, J., Breden, F., ... Dreyer, C.
840 (2010). Genome-wide single nucleotide polymorphisms reveal population history and
841 adaptive divergence in wild guppies. *Molecular Ecology*, 19(5), 968–984. doi:
842 10.1111/j.1365-294X.2010.04528.x
843
844 Wojcik, G. L., Graff, M., Nishimura, K. K., Tao, R., Haessler, J., Gignoux, C. R., ... Carlson, C. S.
845 (2019). Genetic analyses of diverse populations improves discovery for complex traits.
846 *Nature*, 570(7762), 514–518. doi: 10.1038/s41586-019-1310-4
847
848 Wu, P., Wang, K., Zhou, J., Yang, Q., Yang, X., Jiang, A., ... Tang, G. (2019). A genome wide
849 association study for the number of animals born dead in domestic pigs. *BMC Genetics*,
850 20(1), 4. doi: 10.1186/s12863-018-0692-x
851
852 Xiao, Y., Liu, H., Wu, L., Warburton, M., & Yan, J. (2017). Genome-wide Association Studies in
853 Maize: Praise and Stargaze. *Molecular Plant*, 10(3), 359–374. doi:
854 10.1016/j.molp.2016.12.008
855
856 Yang, Jian, Benyamin, B., McEvoy, B. P., Gordon, S., Henders, A. K., Nyholt, D. R., ... Visscher,
857 P. M. (2010). Common SNPs explain a large proportion of the heritability for human
858 height. *Nature Genetics*, 42(7), 565–569. doi: 10.1038/ng.608
859

- 860 Yang, Jinliang, Jiang, H., Yeh, C.-T., Yu, J., Jeddelloh, J. A., Nettleton, D., & Schnable, P. S.
861 (2015). Extreme-phenotype genome-wide association study (XP-GWAS): a method for
862 identifying trait-associated variants by sequencing pools of individuals selected from a
863 diversity panel. *The Plant Journal*, *84*(3), 587–596. doi: 10.1111/tpj.13029
864
- 865 Yoo, A. B., Jette, M. A., & Grondona, M. (2003). SLURM: Simple Linux Utility for Resource
866 Management. In D. Feitelson, L. Rudolph, & U. Schwiegelshohn (Eds.), *Job Scheduling*
867 *Strategies for Parallel Processing* (pp. 44–60). Berlin, Heidelberg: Springer Berlin
868 Heidelberg.
- 869
- 870 Zaitlen, N., Kraft, P., Patterson, N., Pasaniuc, B., Bhatia, G., Pollack, S., & Price, A. L. (2013).
871 Using Extended Genealogy to Estimate Components of Heritability for 23 Quantitative
872 and Dichotomous Traits. *PLoS Genetics*, *9*(5). doi: 10.1371/journal.pgen.1003520
873
- 874 Zappa Nardelli, F., Belyakova, J., Pelenitsyn, A., Chung, B., Bezanson, J., & Vitek, J. (2018).
875 Julia Subtyping: A Rational Reconstruction. *Proc. ACM Program. Lang.*, *2*(OOPSLA),
876 113:1–113:27. doi: 10.1145/3276483
877
- 878 Zhou, X., & Stephens, M. (2012). Genome-wide efficient mixed-model analysis for association
879 studies. *Nature Genetics*, *44*(7), 821–824. doi: 10.1038/ng.2310
880
- 881 Zhu, Y., Bergland, A. O., González, J., & Petrov, D. A. (2012). Empirical Validation of Pooled
882 Whole Genome Population Re-Sequencing in *Drosophila melanogaster*. *PLoS ONE*,
883 *7*(7), e41901. doi: 10.1371/journal.pone.0041901

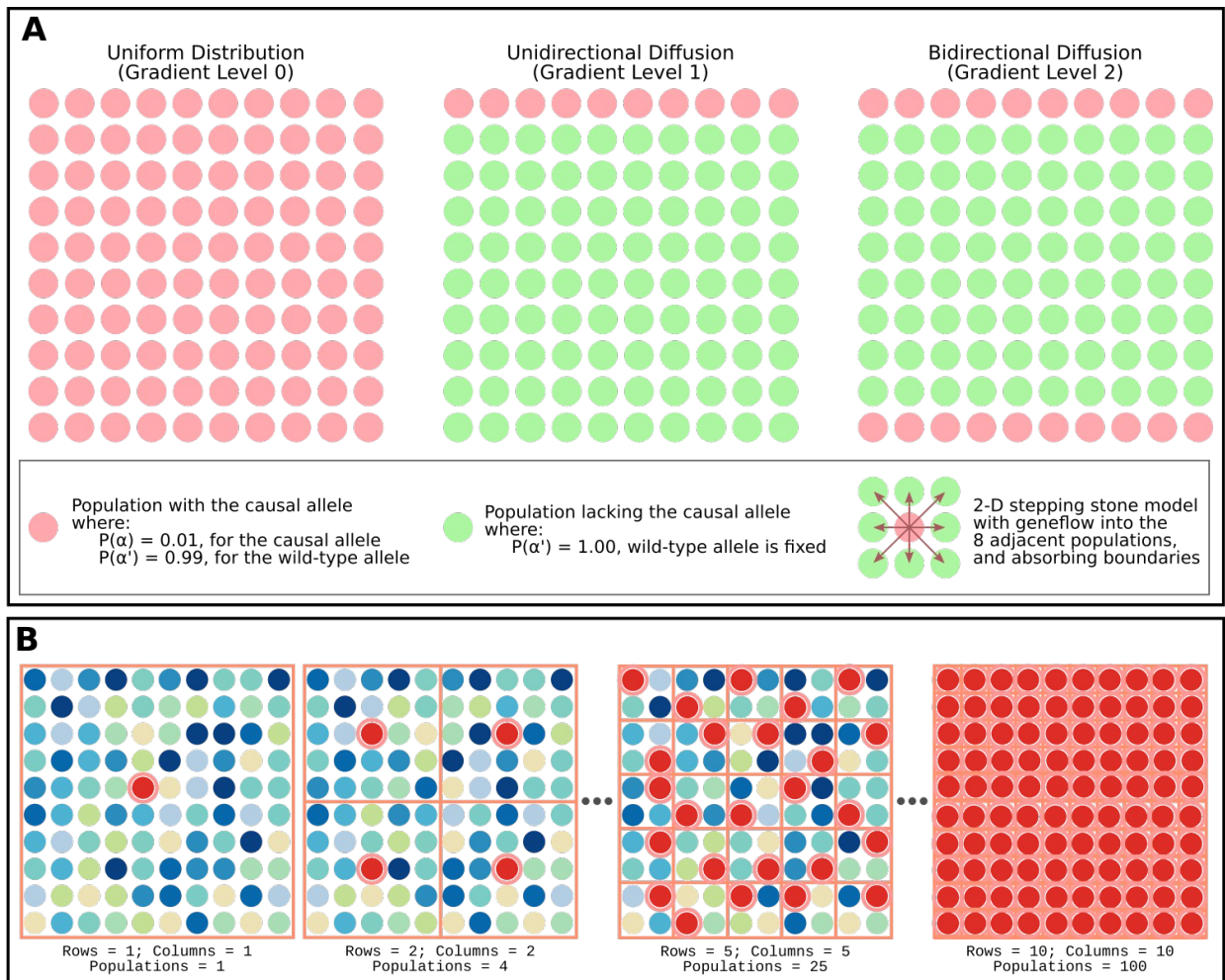
884 **Tables and Figures**

885

886 **Table 1.** List of parameters used in landscape simulations.

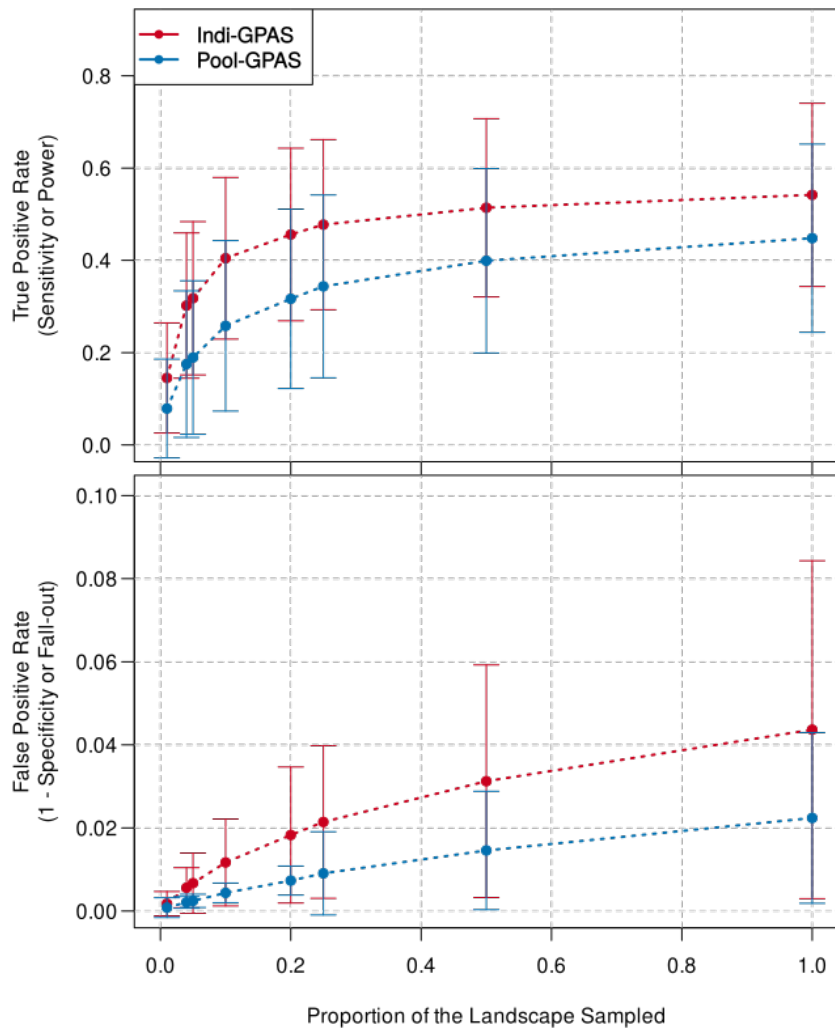
Parameter	Levels
Number of populations per landscape	100
Number of hermaphroditic individuals per population	1,000
Number of loci per individual	10,000
Number of generations	200
Number of loci controlling the trait	10, 50, and 100
Migration rate per population per generation	0.0001, 0.001, and 0.01
Causal allele diffusion gradient	Uniform, unidirectional, and bidirectional
Selection intensity	0.50, 0.90, and 0.95
Number of replicates per landscape	5

887

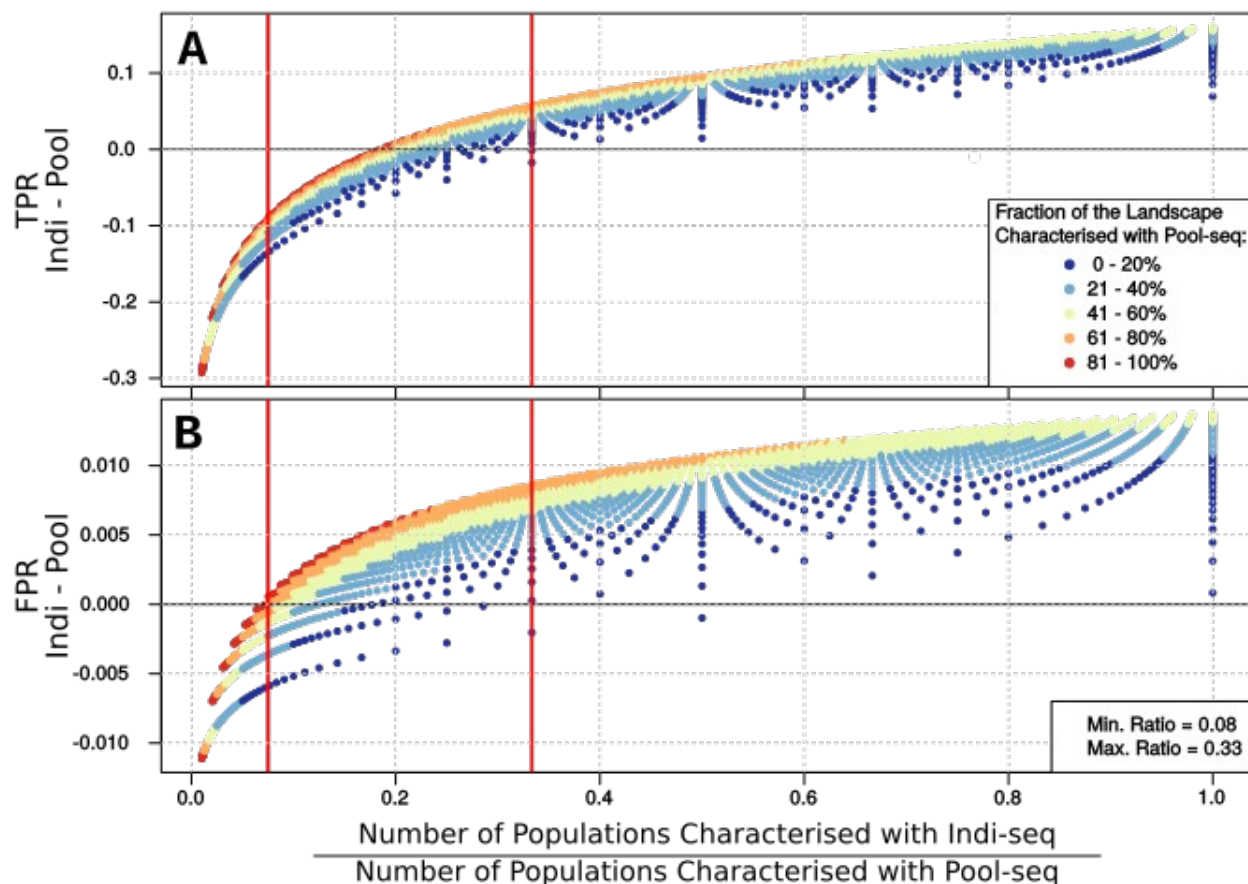


888
 889
 890
 891
 892
 893

Figure 1. Panel A: Causal allele diffusion gradients across the simulated landscape. Panel B: Systematic sampling strategy across the simulated landscape. Note: For one population sampling, all populations across the landscape were sampled independently.

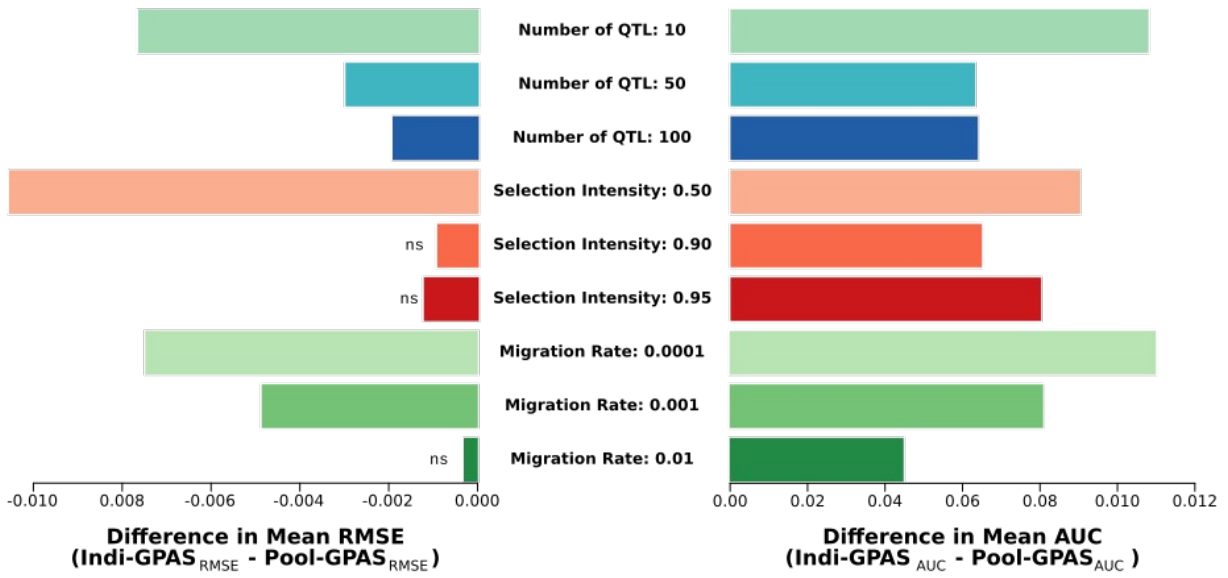


894
 895 **Figure 2.** Relationships between the proportion of the landscape sampled and GPAS
 896 performance. Dots represent means and whiskers indicate ± 1 standard deviation from
 897 the mean.
 898



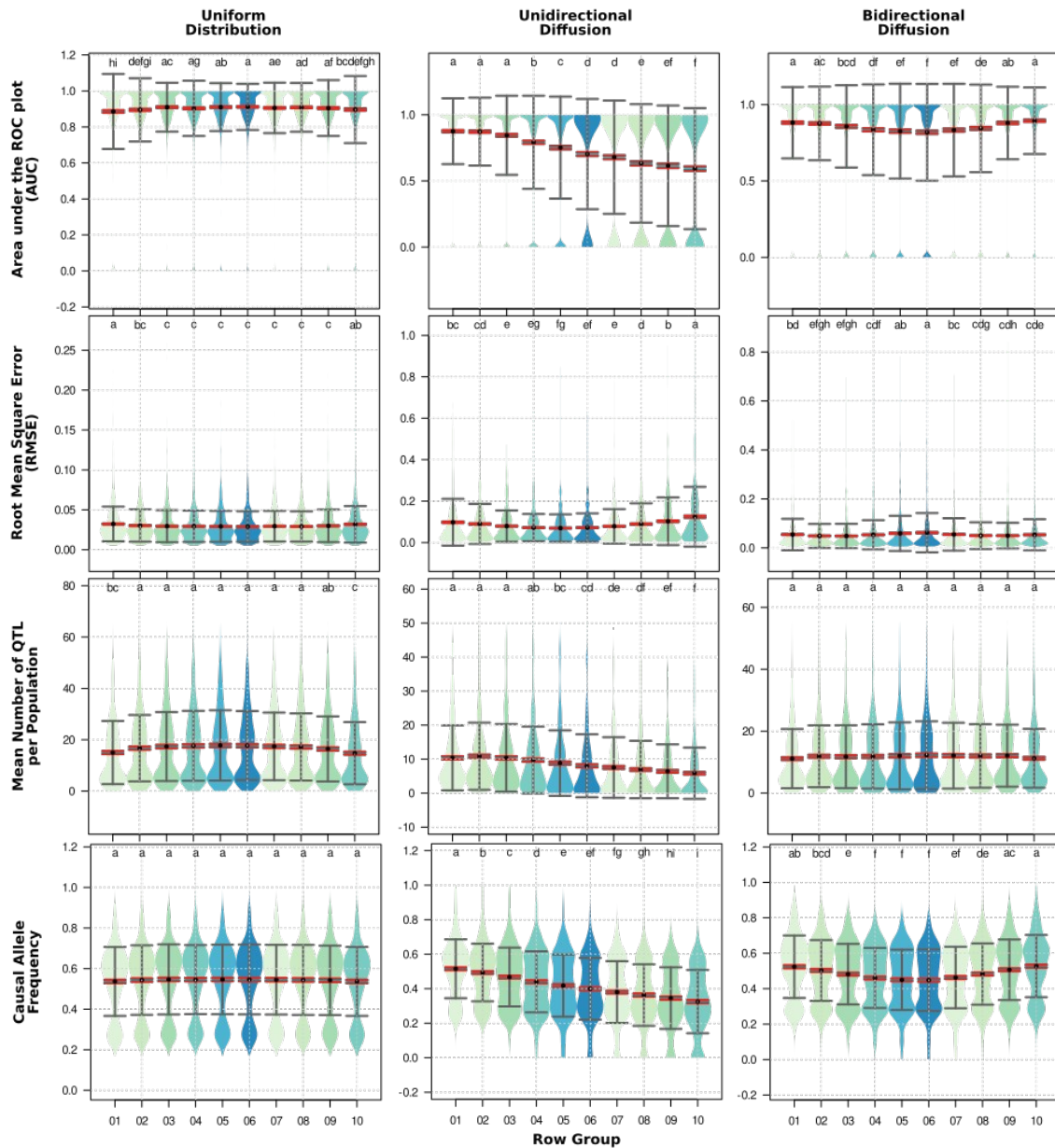
899
 900
 901
 902
 903
 904
 905
 906
 907
 908
 909
 910
 911
 912

Figure 3. Pool-GPAS can outperform Indi-GPAS under the same sequencing capacity. **Panel A:** Difference in true positive rate (TPR) between Indi-GPAS and Pool-GPAS models as the ratio between the number of populations characterised through Indi-seq and Pool-seq increases. **Panel B:** Difference in false positive rate (FPR) between Indi-GPAS and Pool-GPAS models as the ratio between the number of populations characterised through Indi-seq and Pool-seq increases. **Vertical red lines:** The range of ratios between the two vertical red lines correspond to cases when Pool-GPAS can outperform Indi-GPAS in our study, i.e. Pool-GPAS has higher TPR and lower FPR than Indi-GPAS. Moving along the x-axis involves modifying the sequencing depths for Indi-seq or Pool-seq and not the number of individuals or pools sampled per population, since 384 individuals per population and 5 pools per population were kept constant in the simulations.



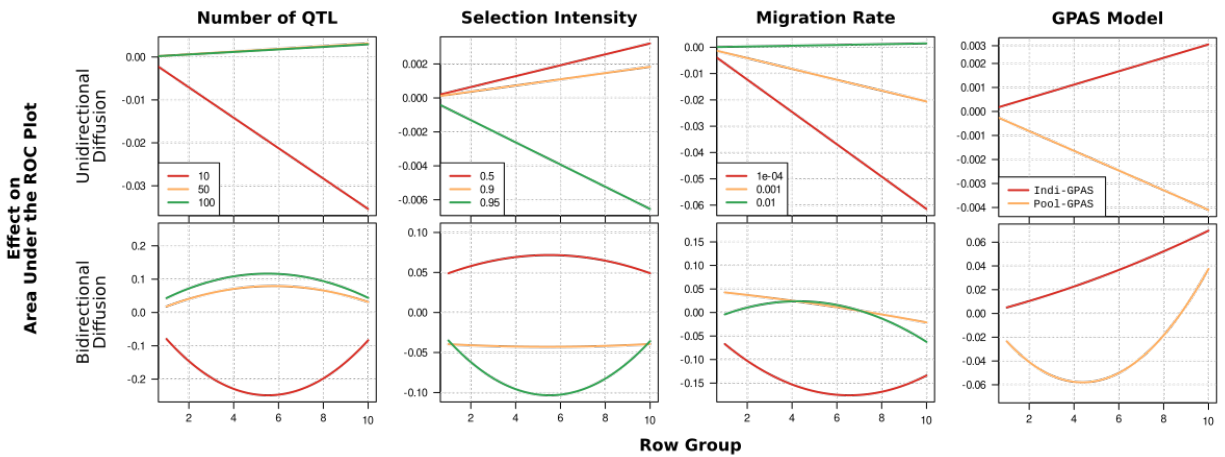
913
914
915
916
917
918

Figure 4. Differences in QTL detection and polygenic score prediction accuracies between Indi-GPAS and Pool-GPAS per population. AUC = Area under the ROC curve. RMSE = root mean square error of the polygenic score prediction. The term “*ns*” beside the bars indicates non-significant differences based on HSD at $p < 0.05$.



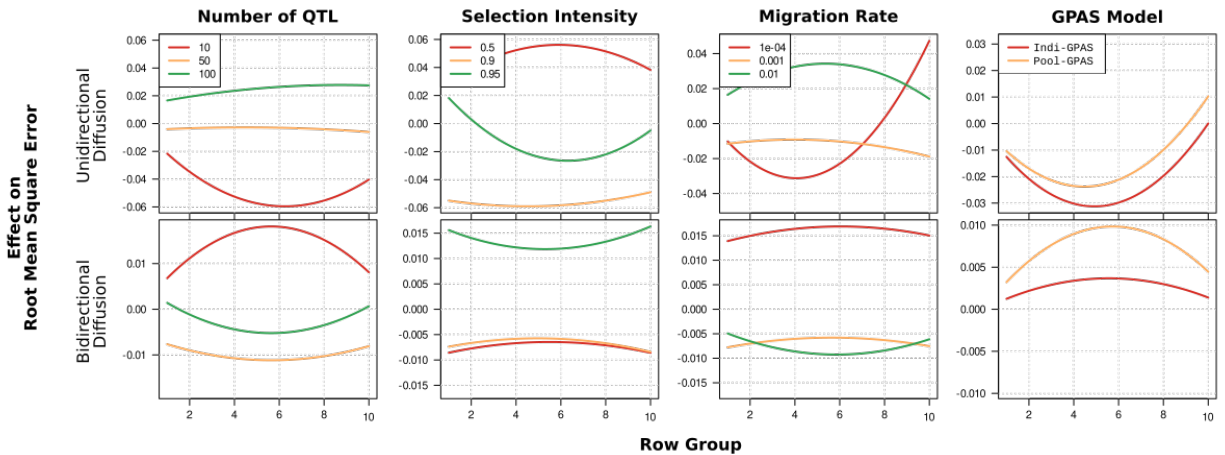
919
 920
 921
 922
 923
 924
 925
 926
 927
 928
 929

Figure 5. Violin plots of the area under the receiver operating curve (AUC; measure of QTL detection accuracy), root mean square error (RMSE; measure of polygenic score prediction accuracy), mean number of polymorphic causal loci per population, and causal allele frequencies across the landscape divided into 10 rows under uniform, unidirectional, and bidirectional causal allele diffusion. Each row is perpendicular to the causal allele diffusion gradient. Black dots represent the mean, black whiskers show ± 1 standard deviation, red whiskers are the 95% confidence interval, and the letters on top of each plot are Tukey's honest significant difference (HSD)-based grouping (i.e. row groups with the same letter are not significantly different at $p < 0.05$).



930
931
932
933
934
935
936
937

Figure 6. Effects of sampling across the landscape on QTL detection accuracy under varying number of simulated QTL, selection intensities, migration rates, and GPAS models for unidirectional (top graphs) and bidirectional (bottom graphs) causal allele diffusion gradients. QTL detection accuracy was measured using the area under the curve which describes the relationship between power and false positive rate, where high values mean high QTL detection accuracies.



938
939
940
941
942
943

Figure 7. Effects of sampling across the landscape on prediction accuracy under varying number of simulated QTL, selection intensities, migration rates, and GPAS models for unidirectional (top graphs) and bidirectional (bottom graphs) causal allele diffusion gradients. Polygenic score prediction accuracy was measured using root mean square error where low values mean high accuracies.